



ISSN: 2617-6548

URL: www.ijirss.com



Evaluation of post liquefaction settlement and treatment and reinforcement of the soil by stone columns

 Mohamed Bziaz^{1*},  Lahcen Bahi²,  Latifa Ouadif³,  Anas Bahi⁴,  Hamou Mansouri⁵,  Abdelhalim Douiri⁶,
 Mimoun Abbach⁷

^{1,2,3,4}GIE Laboratory, Mohammadia Engineering School, Mohammed V University, Rabat, Morocco.

^{5,7}LPEE Public Laboratory for Tests and Studies, Morocco.

⁶Urban Agency of Al Hoceima, Morocco.

*Corresponding author: Mohamed Bziaz (Email: bziazm@gmail.com)

Abstract

During earthquakes, the shear strength and bearing capacity of saturated sandy soils decreases; this is related to an increase in pore pressure. In the ultimate state, the pore pressure becomes equal to the initial effective stress, at which time the material loses all its resistance and liquefaction occurs. Thus, the prediction of the post-liquefaction settlement of the soil is an important step to reduce the seismic risk. Several methods have been developed for the prediction of Seismic-Induced Settlement, the most widely used is that based on the results of in-situ tests SPT, and Several soil reinforcement techniques can be considered, the choice depends mainly on the grain size of the soil to be treated. This article presents a comparative study of the methods for evaluating Seismic-Induced Settlement based on the experimental results of the in situ SPT tests, applied to an earthquake-prone area in northern Morocco which had specific soil formations characterized by the existence of layers of sand over several meters, which suggests the possibility of soil liquefaction and proposes a method of reducing the risk of liquefaction. The analysis of existing SPT data leads to interesting conclusions both in terms of the comparative analysis of methods for the prediction of the post-liquefaction settlement and the understanding of the effect of Soil treatments by Stone Columns to mitigate the risk of liquefaction.

Keywords: Liquefaction, Potential, Prediction, Seismic-Induced settlement, SPT, Stone columns, Treatment.

DOI: 10.53894/ijirss.v6i1.1113

Funding: This study received no specific financial support.

History: Received: 11 August 2022/**Revised:** 1 December 2022/**Accepted:** 20 December 2022/**Published:** 26 December 2022

Copyright: © 2023 by the authors. This article is an open access article distributed under the terms and conditions of the Creative Commons Attribution (CC BY) license (<https://creativecommons.org/licenses/by/4.0/>).

Authors' Contributions: All authors contributed equally to the conception and design of the study.

Competing Interests: The authors declare that they have no competing interests.

Transparency: The authors confirm that the manuscript is an honest, accurate, and transparent account of the study; that no vital features of the study have been omitted; and that any discrepancies from the study as planned have been explained.

Ethical Statement: This study followed all ethical practices during writing.

Publisher: Innovative Research Publishing

1. Introduction

Soil liquefaction is a serious problem capable of causing often irreparable damage, both to existing works and to new constructions, the soils likely to liquefy under cyclic loading being silty to sandy. Several earthworks have been severely damaged in past earthquakes, including in Japan during the Tōhoku earthquake of March 11, 2011 (magnitude 9.0). One of the phenomena responsible for much damage is the liquefaction of soils under cyclic loading. The phenomenon of liquefaction concerns certain geological formations, defined by their nature (sands, silts, muds), their cohesion (not very compact formations), their degree of water saturation (the formation must be saturated with water), their grain size (uniform grain size, included between 0.05 and 1.5 mm). Several studies have been undertaken since 1964 to understand the risk of liquefaction and assess its consequences. The occurrence of liquefaction in soils is often assessed following the simplified method based on the Standard Penetration Test (SPT). The Prediction of the liquefaction potential of the soil as well as the post-liquefaction settlement is an important step in judging the most suitable soil treatment to mitigate the risk of soil liquefaction.

In this article, a detailed study was carried out on an area located in the north of Morocco (Nekkour Basin) characterized by the existence of sandy deposits which are liable to liquefy. This study consists of the verification of the risk of liquefaction, the evaluation of liquefaction potential and Seismic-Induced Settlement, and finally the choice of the most suitable treatment to mitigate the risk of liquefaction and improve soil characteristics.

2. Methodology

2.1. Assessment of Liquefaction Risk

In the presence of groundwater, the resistance to liquefaction of the soil is evaluated by applying the NCEER (National Center for Earthquake Engineering Research) method, developed by Youd and Idriss [1]. Equation 1 presents the safety factor of soil liquefaction:

$$LSF = CRR/CSR \quad (1)$$

With:

CSR: cyclic stress ratio.

CRR: cyclic resistance ratio.

According to EN 1998-5 [2] and RPS [3], liquefaction occurs if the ratio:

$$CRR/CSR < 1.25 \quad (2)$$

2.1.1. Cyclic Stress Ratio (CSR) Assessment

Seed and Idriss [4] formulated the following equation for the calculation of the cyclic stress ratio CSR

$$CSR = \frac{\tau_{av}}{\sigma'_{v0}} = 0.65 \left(\frac{\alpha_{max}}{g} \right) \left(\frac{\sigma_{v0}}{\sigma'_{v0}} \right) r_d \quad (3)$$

Where τ_{av} is the average cyclic shear stress; α_{max} is the maximum horizontal acceleration at the ground surface; $g = 9.81 \text{ m}^2 / \text{s}$ is the acceleration due to gravity; σ_{v0} is the initial vertical total stress; σ'_{v0} is the initial effective vertical stress; r_d is the stress reduction factor. The stress reduction coefficient is expressed as a function of depth by the following equations [5]:

$$r_d = 1 - 0.00765z \quad z \leq 9.15\text{m} \quad (4)$$

$$r_d = 1.74 - 0.0267z \quad 9.15\text{m} < z \leq 23\text{m} \quad (5)$$

2.1.2. Evaluation of Cyclic Resistance Ratio (CRR) [6-8]

The determination of cyclic soil resistance can be carried out using data obtained from in-situ tests (Standard penetration test, Cone penetration test, shear wave velocity measurement). To incorporate the effect of earthquake magnitude (duration of earthquake or number of cycles), an MSF magnitude correction factor that adjusts the CRR value to an earthquake magnitude of 7.5 will be added in the following equation which becomes as follows:

$$CRR = CRR_{7.5} * CM \quad (6)$$

With CM: correction factor, determined according to EN 1998-5 (2004) (English) [2] based on surface wave amplitude M.

Table 1 presents the Correction factor (CM), determined according to Annex B of EN 1998-5 standard [2], based on the magnitude of surface waves (M).

Table 1. Correction factor (CM), determined according to annex B of EN 1998-5 standard [2], based on the magnitude of surface waves (M).

M	CM
5.50	2.86
6.00	2.20
6.50	1.69
7.00	1.30
8.00	0.67

Note: (CM: Correction factor), (M: Magnitude of surface waves).

The standard penetration test is the most commonly used test. It consists of determining the number of strokes N necessary to sink a corer to a depth of 30 cm while taking reworked samples indicative of the different layers crossed. This

method uses the normalized standard penetration index $N_{1.60cs}$ where the index notation associated with the value of N has the following meaning.

1: indicates a normalized value for a load of one atmosphere (100 kPa).

60: indicates a normalized value for an efficiency of 60% of the total energy supplied by the hammer.

cs: indicates a normalized value for clean sand (clean sand), i.e. without fine particles.

In the case of clean sand, the standard penetration index $N_{1.60}$ can be determined as follows [Youd and Idriss \[1\]](#) the corrected number of blows is determined by:

$$N_{1.60} = Nm \cdot CN \cdot CE \cdot CB \cdot CR \cdot CS \quad (7)$$

Nm : Number of strokes measured.

CN : Correction factor for the effective confining stress (depending on the depth), according to [Liao and Whitman \[5\]](#):

$$CN = \min ((Pa / \sigma'_{v0})^{0.5} ; 1.7) \quad (8)$$

C_E : Correction factor for the energy transmitted by the hammer,

$$CE = ER / 60 \quad ER = 100 \times \text{specific energy ratio of equipment (\%)} \quad (9)$$

C_B : Correction factor for borehole diameter

$$65 < D < 115 \text{ mm} \rightarrow CB = 1$$

$$115 < D < 200 \text{ mm} \rightarrow CB = 1.05 \quad (10)$$

$$D > 200 \text{ mm} \rightarrow CB = 1.15$$

C_R : Correction factor for the length of the rods (depth of the hole),

$$L < 3 \text{ m} \rightarrow CR = 0.75$$

$$3 < L < 4 \text{ m} \rightarrow CR = 0.8$$

$$4 < L < 6 \text{ m} \rightarrow CR = 0.85 \quad (11)$$

$$6 < L < 10 \text{ m} \rightarrow CR = 0.95$$

$$L > 10 \text{ m} \rightarrow CR = 1$$

C_S : Correction factor for the sampling method. Standard sampler $\rightarrow CS = 1 \quad (12)$

Sampler without liners $\rightarrow CS = 1.1$ to 1 .

If fine particles are present, the following correction must also be made [\[1\]](#).

$$N_{1.60cs} = \alpha + \beta \cdot N_{1.60} \quad (13)$$

The coefficients are a function of the percentage of fine particles by mass (or Fines content –FC) corresponding to the passage of the #200 sieve. They take the following values depending on the case [\[1\]](#).

$$\begin{cases} \alpha = 0 \\ \beta = 1 \end{cases} \text{ Pour } FC \leq 5\% \quad (14)$$

$$\begin{cases} \alpha = \exp(1.76 - (190/FC^2)) \\ \beta = (0.99 + (FC^{1.5}/1000)) \end{cases} \text{ Pour } 5\% < FC < 35\% \quad \begin{cases} \alpha = 5 \\ \beta = 1.5 \end{cases}$$

$$\text{ Pour } FC \geq 35\% \quad CRR_{M,\sigma'_v} = CRR_{M=7.5,\sigma'_v=1} \cdot MSF \cdot K_\sigma \quad (15)$$

MSF Magnitude correction factor.

K_σ The effective confinement stress is the earth weight correction factor applied to [Idriss and Boulanger \[9\]](#); [Youd and Idriss \[1\]](#). revised the value of K_σ :

$$K_\sigma = 1 - (Pa) \leq 1 \quad (16)$$

$$C_\sigma = 1 - 18.9 - 2.55 \sqrt{(N1)60} \quad (17)$$

C_σ : Correction factor ($C_\sigma < 0.3$)

$(N1)60$: the corrected value of N_{spt}

For a magnitude of 7.5, an approximation of CRR is given by the following formula: [Idriss and Boulanger \[8\]](#)

$$CRR_{7.5} = \text{EXP} \left[\frac{(N1)_{60cs}}{14.1} + \left(\frac{(N1)_{60cs}}{126} \right)^2 - \left(\frac{(N1)_{60cs}}{23.6} \right)^3 + \left(\frac{(N1)_{60cs}}{25.4} \right)^4 - 2.8 \right] (N1)_{60cs} = (N1)_{60} + \text{EXP} \left(1.63 + \frac{9.7}{FC+0.1} - \left(\frac{15.7}{FC+0.1} \right)^2 \right) \quad (18)$$

2.2. Prediction of Seismic-Induced Settlement

2.2.1. Tokimatsu and Seed [10]

The method proposed by [Tokimatsu and Seed \[10\]](#) is limited to cases where there is no liquefaction (LSF : liquefaction safety factor > 1) but is easy to use because it only requires knowledge of the liquefaction safety factor. This method uses data from the SPT $(N1)60$ and the cyclic stress induced by an earthquake of magnitude $M=7.5$ (C.S.R.).

2.2.2. Method of Ishihara and Yoshimine [11]

The method proposed by [Ishihara and Yoshimine \[11\]](#): settlement is linked to the maximum value of distortion and the value of the initial relative density of the sand. The evaluation of the volumetric deformation ϵ_v can be made using the abacus of [Ishihara and Yoshimine \[11\]](#) modified by [Idriss and Boulanger \[8\]](#) ([Figure 1](#)), from the liquefaction safety factor LSF and another parameter selected from among the following: soil relative density D_r , normalized SPT resistance $(N1)60$, normalized penetration resistance q_{c1N} , or maximum distortion induced by the earthquake γ_{max} . Once the volumetric deformation ϵ_v has been evaluated at each depth, the settlement of the surface during the dissipation of the pore pressures generated by the earthquake is estimated by multiplying its thickness for each layer by its volumetric deformation ϵ_v . These simplified methods commonly used by engineering are limited to a well-defined range of sandy materials: clean sands; the values of SPT $(N1)60$ covered by this chart are between 4 and 37 and the values of q_{c1N} are between 60 and 235 [\[12\]](#). They are also based on historical observations of seismic-induced settlement.

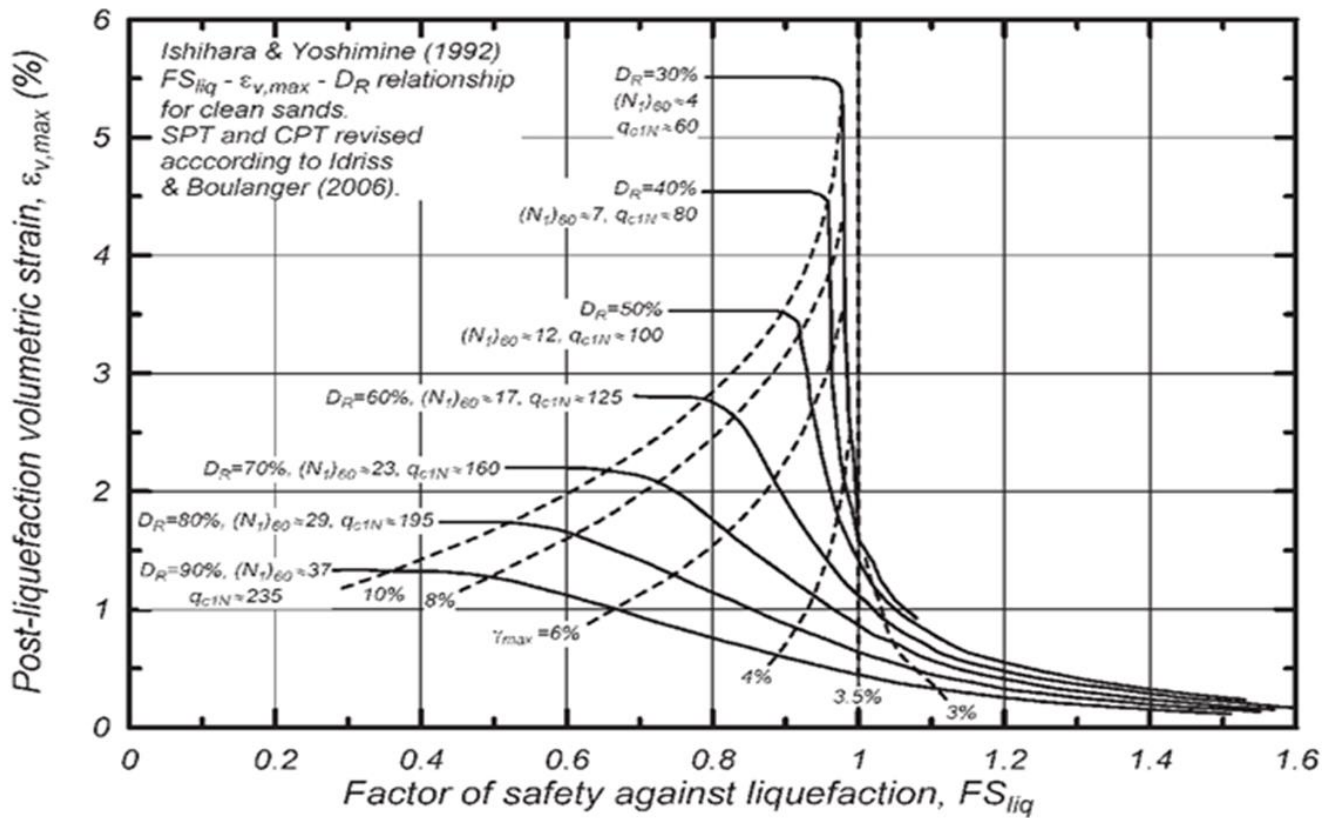


Figure 1. Volume deformation ϵ_v as a function of the liquefaction safety factor ($r_u=100\%$) for clean sands with variable initial relative densities [8].

2.2.3. Method of Zhang, et al. [13]

The empirical relationship between the post-liquefaction volumetric strain and the peak resistance $(qc1N)_{cs}$ is given by the equations below based on the curves of Ishihara and Yoshimine [11].

$$\epsilon_v = \alpha (qc1N)_{cs}^\beta \quad (19)$$

$$(qc1N)_{cs} = 0.0059(N1_{60cs})^3 - 0.1479(N1_{60cs})^2 + 5.2189(N1_{60cs}) + 18.087 \quad (20)$$

Table 2 presents the empirical relationship between the deformation post-liquefaction volume and normalized peak resistance for a "clean sand" equivalent $(qc1N)_{cs}$, For a previously calculated safety factor.

Table 2. The empirical relationship between the deformation post-liquefaction volume and normalized peak resistance for a "clean sand" equivalent $(qc1N)_{cs}$, For a previously calculated safety factor.

LSF ≤ 0.5	$(qc1N)_{cs} \leq 200$	$\alpha = 102 ; \beta = -0.82$
LSF ≤ 0.6	$(qc1N)_{cs} \leq 147$	$\alpha = 102 ; \beta = -0.82$
LSF ≤ 0.6	$147 < (qc1N)_{cs} \leq 200$	$\alpha = 2411 ; \beta = -1.45$
LSF ≤ 0.7	$(qc1N)_{cs} \leq 110$	$\alpha = 102 ; \beta = -0.82$
LSF ≤ 0.7	$110 < (qc1N)_{cs} \leq 200$	$\alpha = 1701 ; \beta = -1.42$
LSF ≤ 0.8	$(qc1N)_{cs} \leq 80$	$\alpha = 102 ; \beta = -0.82$
LSF ≤ 0.8	$80 < (qc1N)_{cs} \leq 200$	$\alpha = 1690 ; \beta = -1.46$
LSF ≤ 0.9	$(qc1N)_{cs} \leq 60$	$\alpha = 102 ; \beta = -0.82$
LSF ≤ 0.8	$60 < (qc1N)_{cs} \leq 200$	$\alpha = 1430 ; \beta = -1.48$
LSF ≤ 1.0	$(qc1N)_{cs} \leq 200$	$\alpha = 64 ; \beta = -0.93$
LSF ≤ 1.1	$(qc1N)_{cs} \leq 200$	$\alpha = 11 ; \beta = -0.65$
LSF ≤ 1.2	$(qc1N)_{cs} \leq 200$	$\alpha = 9.7 ; \beta = -0.69$
LSF ≤ 1.3	$(qc1N)_{cs} \leq 200$	$\alpha = 7.6 ; \beta = -0.71$
LSF > 1.3		$\epsilon_v = 0.00$

2.2.4. Method of the SLAKE Program [14]

The Slake program includes an additional calculation option derived from the simplified "NCEER" procedure, taking into account certain adaptations from the recommendations of Cahier Technique no. 45 of the FAPE (The French Association of Paraseismic Engineering) "Assessment of the risk of liquefaction of soils under the effect of earthquakes - Practical knowledge and applications to geotechnical projects" (calculation option NCEER/CT45- AFPS [14]). Adjustments have been

made to the following coefficients: * MSF: (Magnitude Scaling Factor) which makes it possible to take into account the real magnitude of the earthquake and to combine the effects of the confinement pressure and stress inclination.

2.3. Prediction of the Liquefaction Potential Index

Iwasaki, et al. [15] propose to extend the concept of safety factor FS vis-à-vis the Liquefaction hazard, calculated in a discrete way at each point of a sounding, to a global parameter Characterizing the entire column of soil examined by sounding (SPT or CPT(u)) via the introduction of a liquefaction index (liquefaction potential index, LPI). This is determined by integrating severity indices(z) (to be distinguished from safety factors SF(z) over 20m_depth beyond which the risk is considered negligible by the authors by associating them with a weighting function w(z) driving the decrease of the relative importance of SF in depth

$$LPI = \int_0^{20} F(z) \omega(z) dz \quad \text{Avec}$$

$$LSF(z) < 1.0 \quad = F(z)$$

$$= 1 - FS$$

$$LSF(z) > 1.0$$

$$F(z) = 0$$

$$\text{And } \omega(z) = 10 - 0.5z$$

2.3.1. Dhouib and Blondeau [16]

Based on the curves of Ishihara and Yoshimine [11], Driss & Boulanger proposed the following empirical relationship:

$$\varepsilon_v = 1.5e^{(-0.025Dr,ini)} \cdot \min \{8; y_{max}\} \quad Dr,ini = \sqrt{\frac{N1(60)cs}{46}}$$

$$\text{If } Dr,ini \geq 39.2\% \Rightarrow F_{ult} = 0.032 + 0.047 \cdot Dr,ini - 0.0006 \cdot (Dr,ini)^2$$

$$iF_{notFult} = +0.9524$$

$$\text{If } LSF < F_{ult} \Rightarrow y_{max} \rightarrow \infty$$

$$\text{If } LSF > 2 \Rightarrow y_{max} = 0$$

$$\text{If } F_{ult} \leq FS \leq 2 \Rightarrow y_{max} = 3.5 (2 - LSF)^{\left(\frac{1 - F_{ult}}{FS - F_{ult}}\right)}$$

Several authors have, on this basis, established a scale of the qualitative hierarchy of the hazard which proposes the following qualification of the hazard at the right of a sampling point from the exploitation of the LPI index: $0 < LPI \leq 2 \Rightarrow$ Low risk.

$2 < LPI \leq 5 \Rightarrow$ Moderate risk.

$5 < LPI \leq 15 \Rightarrow$ High risk.

$LPI > 15 \Rightarrow$ Very high risk.

2.4. Effect of Stone Columns on Reducing the Risk of Liquefaction [16]

The stone column is particularly well suited in heterogeneous soils to reduce the risk of liquefaction. Indeed, it can intervene on several parameters at the same time (liquefiable material, reduction of seismic stresses, modification of the state of stress in the soil). The stabilizing effect of the stone column is based on its high shear strength and its ability to dissipate pore pressures very quickly in its immediate environment. The high permeability of the gravel of the columns allows the rapid reduction of pore pressures.

3. Study of a Case (Nekkour Basin in the City of Al-Hoceima)

Our case study is located in northern Morocco in the city of Al Hoceima, precisely, the area of Souani.

3.1. Geological Setting

The lands of the municipality of Al Hoceima are predominated by outcrops of carbonate rocks of the Ghomarides and internal limestone ridge, which are in the form of massive limestone dolomites with outcrops of shale and marl-sandstone formations. This context is delimited via abnormal contacts (overthrust and stacking) to the East, South, and West by a Liassic unit of limestone with flint and microbreccias containing levels of limestone, dolomites, and radiolarites, to the Northwest by a block of massive Triassic dolomite and to the north by the Paleozoic unit presented by limestones from the Tirhanimine and the southern tip of Al Hoceima. These units are covered in places by lands of recent Quaternary cover.

3.2. The Seismicity of the Region

The province of Al Hoceima is part of the Rif chains, this region is the seat of a very active instrumental seismic activity, which has been verified and validated by a set of studies that have highlighted the existence of numerous structures active within the Riffian chains. This seismic activity is also notable through the historical seismicity as evidenced by the earthquake of May 26, 1994, in the region of Al-Hoceima, aspens under the effect of an earthquake of magnitude $M_w = 5.8-6$ destroying many habitats in the city of Al -Hoceima and in the surrounding countryside. Ten years later, on February 24, 2004, a deadly earthquake of magnitude $M_w = 6.3-6.5$ also occurred in the same province, leading to the death of more than 600 people and the destruction of 2,500 homes. This earthquake is felt more than 300 km from the epicenter. In addition, the region of Al Hoceima is part of zone No. 3 according to the RPS 2000 revised in 2011, and therefore a maximum acceleration of 0.14 g is considered.

Figure 2 shows the SPT tests carried out in this area.



Figure 2.
The SPT tests carried out in this study area.

3.3. In-Situ Tests

11 SPT tests were carried out. Given the number of tests that were carried out, a detailed example will be carried out for a single SPT test. For the other tests, we simply use the final result.

4. Results and Discussions

4.1. Evaluation of Liquefaction Potential and Seismic-Induced Settlement

We evaluate the liquefaction potential and the seismic-induced settlement by the three methods using data from the SPT test surveys carried out in the SOUANI Province of the Al Hoceima area. the results are presented below, for this zone ($X=641556$, $Y=511452$) we take: $CE=CB=CR=CS=1$ and $amaxg = 0.22$ g $CM=1.3$

N -table water(m)=2 δt (KN/m3)=20 $Mw=7$ δw (KN/m3)=10 . Given the number of tests carried out, the detailed calculation will be carried out for a single test (Table 3), for the other tests, we are satisfied only with the final result of the liquefaction potential and the seismic-induced settlement Table 4.

It can be seen that the three methods provide almost the same values for the liquefaction intensity for the nine boreholes, for the P1 and P2 boreholes the SLAKE program provides greater values. With regard to post-liquefaction settlement, the values found by the Zhang, et al. [13] method are close to the averages of the three methods and are framed by the values found by the other two methods [6] SLAKE program), for each survey if a value of one of these last two methods is higher than the value found by the method [13] the other value is lower and vice versa. It can be seen that most of the depths are affected by a high risk of liquefaction at ground level, hence the need to improve their characteristics.

Table 3. Calculation of safety factor, liquefaction potential index, and seismic-induced settlement for SPT1 by the three methods.

Z(m)	CSR	N1(60)cs	CRR	LSF	Zhang, et al. [13]			Dhouib and Blondeau [16]			SLAKE program			The average						
					(qc1N)cs	LPI	ε _v	Dr.ini	Fult	γ _{max}	LPI	ε _v	Sett	LPI	ε _v	Sett	LPI	ε _v	Sett	
2.5	0.16	10.05	0.15	0.99	61.59	12.25	1.39	42.22	0.467	0.054	3.59	12.25	1.67	36.35	16.63	4.39	46.88	13.71	2.48	41.82
3.5	0.18	21.13	0.29	1.62	118.00		0.00		0.678	0.064	0.81		0.22			3.98			1.40	
4.5	0.19	14.77	0.20	1.05	81.89		0.63		0.567	0.058	3.17		1.15			3.97			1.92	
5.5	0.20	8.46	0.14	0.70	55.22		3.80		0.429	0.052	6.72		3.45			3.92			3.72	
6.5	0.21	11.50	0.17	0.81	67.52		2.80		0.500	0.055	5.26		2.26			3.82			2.96	
7.5	0.21	12.85	0.18	0.85	73.26		2.48		0.529	0.057	4.76		1.91			3.79			2.73	
8.5	0.22	9.37	0.15	0.68	58.84		3.61		0.451	0.053	6.97		3.38			3.71			3.57	
9.5	0.22	11.21	0.16	0.75	66.31		3.27		0.494	0.055	5.96		2.60			3.54			3.14	
10.5	0.21	10.98	0.16	0.74	65.37		3.31		0.489	0.055	6.03		2.67			3.47			3.15	
11.5	0.21	9.92	0.15	0.71	61.06		3.50		0.464	0.054	6.55		3.08			3.46			3.35	
12.5	0.21	8.94	0.14	0.68	57.13		3.70		0.441	0.053	7.02		3.50			3.31			3.50	
13.5	0.20	9.52	0.14	0.71	59.45		3.58		0.455	0.053	6.47		3.11			2.96			3.22	
14.5	0.20	9.45	0.14	0.72	59.18		3.59		0.453	0.053	6.30		3.04			0.88			2.51	
15.5	0.19	13.87	0.18	0.94	77.78		1.12		0.549	0.058	3.93		1.49			0.83			1.15	
16.5	0.19	15.11	0.19	1.03	83.52		0.62		0.573	0.059	3.29		1.18			0.49			0.76	
17.5	0.18	12.70	0.17	0.93	72.61		1.19		0.525	0.057	4.02		1.62			0.37			1.06	
18.5	0.18	32.84	0.84	2.50	238.87		0.00		0.845	0.071	0.00		0.00			0.00			0.00	

Note:(Z(m): Depth), (CSR: Cyclic stress ratio), (N1(60)cs: Normalized standard penetration index), (CRR: Cyclic resistance ratio), ((qc1N)cs: Normalized peak resistance), (ε_v : Post-liquefaction volumetric strain), (Sett: Seismic-induced settlement), (Dr.ini: The initial relative density),(Fult: Term depends on Dr.in)i,(γ_{max}: Maximum distortion), (LPI: Liquefaction potential index), (LSF: Factor safety).

Table4. Calculation of liquefaction potential index and seismic-induced settlement for the 11 boreholes.

Location	X	Y	Zhang, et al. [13]		Idriss and Boulanger [6]		SLAKE program		The average	
			LPI	Sett	LPI	Sett	LPI	Sett	LPI	Sett
SPT1	641556	511452	12.25	42.22	12.25	36.35	16.63	46.88	13.71	41.82
SPT2	643010	511767	10.40	43.66	10.40	41.19	12.23	51.14	11.01	45.33
SPT3	643972	510333	6.28	30.21	6.28	30.24	6.33	32.42	6.30	30.96
SPT4	644881	508641	2.40	18.53	2.40	22.17	1.94	17.66	2.25	19.45
SPT5	643239	508472	6.08	30.30	6.08	28.55	6.08	32.72	6.08	30.53
SPT6	642447	510514	5.19	28.18	5.19	28.65	5.19	33.69	5.19	30.17
SPT7	643702	507299	2.82	11.63	2.82	12.78	2.16	13.76	2.60	12.72
SPT8	638709	510150	9.09	42.90	9.09	36.60	9.09	50.04	9.09	43.18
SPT9	638257	511006	2.66	10.77	2.66	14.42	3.08	12.11	2.80	12.43
SPT10	641123	509420	5.80	20.89	5.80	19.39	7.01	27.65	6.20	22.64
SPT11	642382	507667	9.96	37.57	9.96	27.71	10.75	40.14	10.22	35.14

Note: ((X,Y) : Lambert coordinates), (LPI: Liquefaction potential index), (Sett: Seismic-induced settlement).

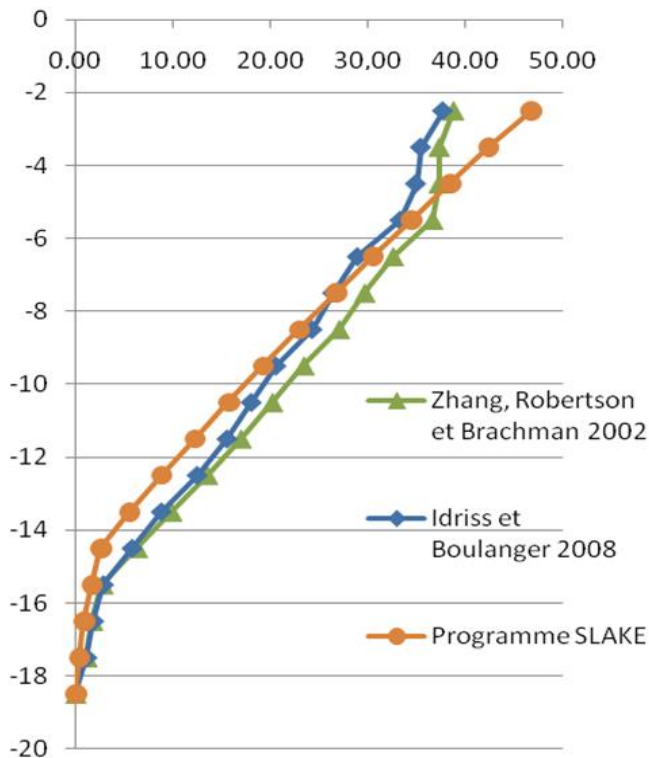


Figure 3. Seismic-induced settlement as a function of depth by the three methods for the P1 borehole.

Figure 3 illustrates the Seismic-induced settlement as a function of depth by the three methods for the P1 borehole.

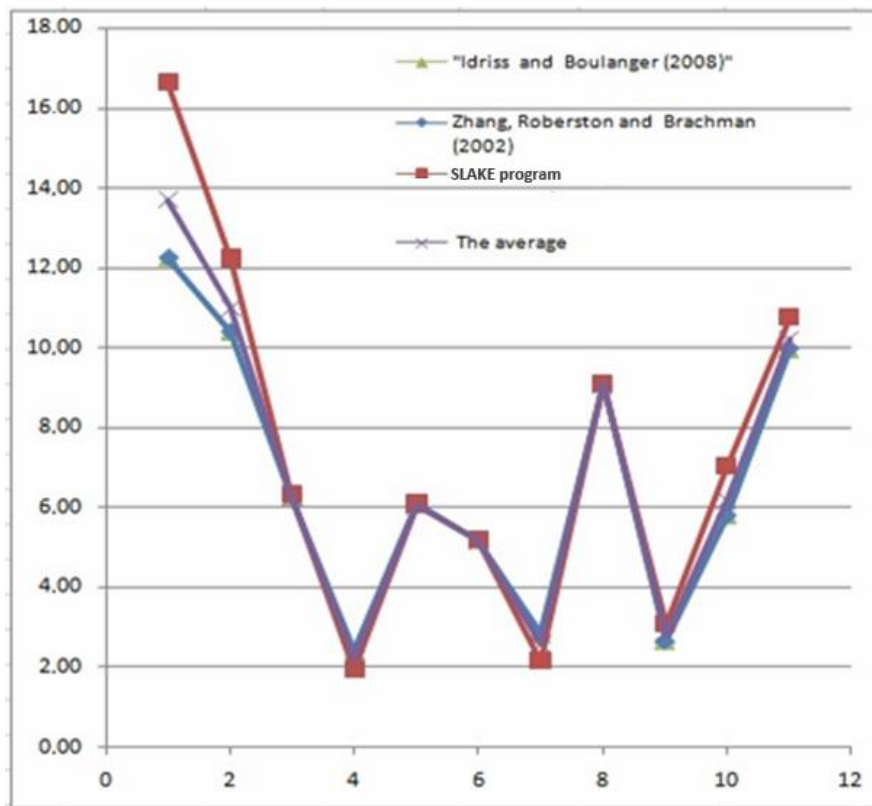


Figure 4. Liquefaction intensity for the 11 boreholes for the three methods.

Figure 4 illustrates the Liquefaction intensity for the 11 boreholes for the three methods.

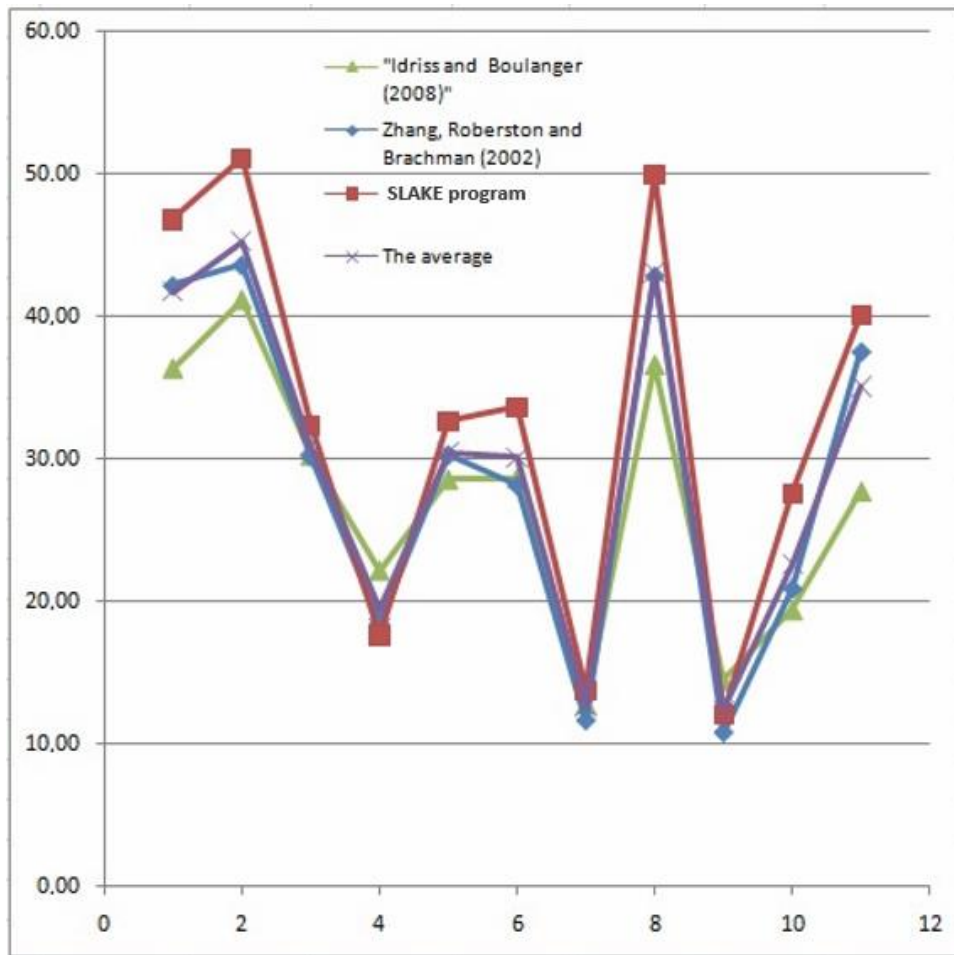


Figure 5. Post-liquefaction settlement for the 11 boreholes for the three methods.

Figure 5 illustrates the Post-liquefaction settlement for the 11 boreholes for the three methods.

4.2 Relationship between Liquefaction Intensity and Seismic-Induced Settlement

Using the results of the liquefaction intensity and the seismic-induced settlement, a relationship can be established between the two series using the linear regression method, this relationship can be written in the following linear form: $y = 2.51x + 12.24$ Seismic-induced settlement = $2.51 * (\text{Liquefaction intensity}) + 12.24$.

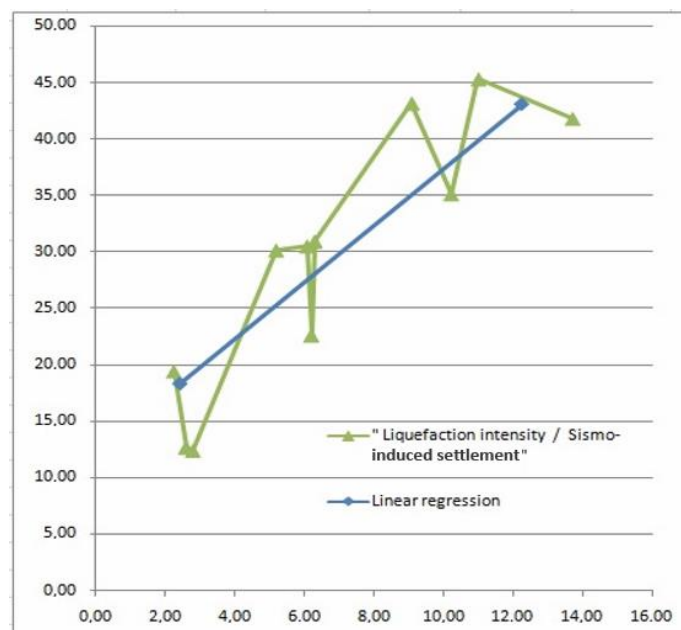


Figure 6. Relation Liquefaction intensity and seismic-induced settlement.

Figure 6 illustrates the Relation between Liquefaction intensity and seismic-induced settlement.

4.3. Soil Treatments: Evaluation of the Attenuation of Liquefaction by Stone Columns

Stone columns have a significant capacity to dissipate pore pressures. Unlike a drain, the stone column is made of a highly permeable compacted gravel material. Its high capacity to evacuate pore pressures results from its high permeability, and also the appearance during the earthquake of a strong hydraulic gradient, linked to the phenomenon of dilatancy of the gravel of the columns [17]. To assess the risk reduction of the liquefaction potential, we use the method of Seed and Booker [18] which is based on the dissipation of excess pore pressure [19]. According to the RPS 2000 version 2011 [3], to have a safety factor greater than 1.33, it is necessary to find a ratio $r_{u\max} = U / v_0' < 0.6$ (U: Interstitial pressure, v_0' : Initial effective stress) This ratio ($r_{u\max}$) is deduced from Figure 7.

We have

Neq: Number of equivalent seismic cycles, defined in Table 5 (Neq = 8 for a zone of average seismicity).

Nl: Number of cycles leading to liquefaction, deduced from the nomogram in Figure 8[2] (Nl=8).

Therefore $Neq/Nl = 1$

We have also

a: Radius of the stone column, (a = 0.4 m).

b: Radius of influence of the column, for the square grid, $b = 1.13 * I / 2$, where I is the spacing, (I = 1.7m and b = 0.960 m) Therefore $a / b = 0.42$

For Tab which is a dimensionless parameter defined by the following formula:

$$Tab = (Ks.td)/(mv.a^2.\gamma_w)$$

Where:

Ks: horizontal soil permeability (Ks=10-5 m/s).

td: Duration of the earthquake (td = 14s for an area of average seismicity).

γ_w : Water density

mv: Soil compressibility $mv = 1 / E_{oed}$ By correlation.

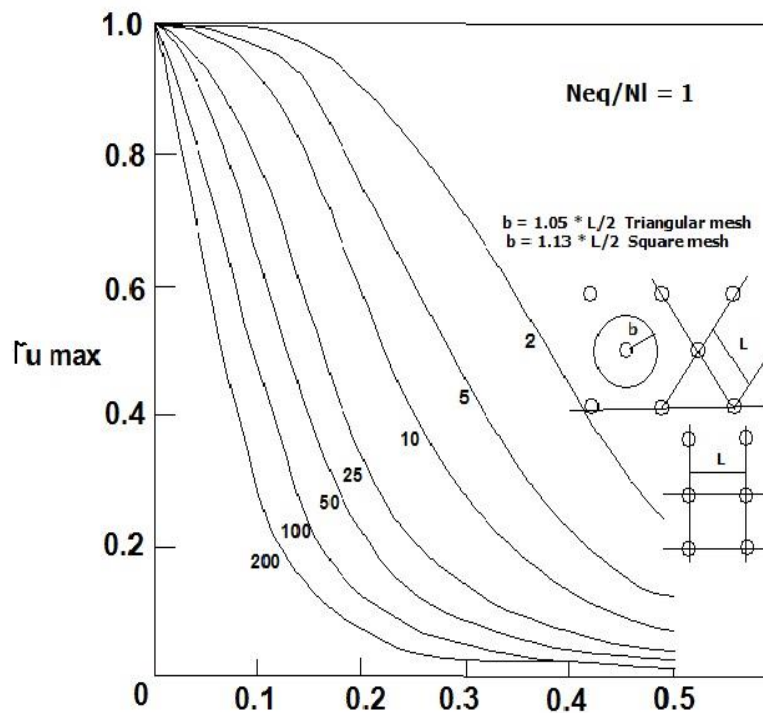


Figure 7. Determination of a/b ratio (a = drain radius and b = half spacing) [20].

Table 5. Number of equivalent cycles and duration of the earthquake according to the seismic zone [19].

Seismicity zone	Conventional magnitude	Number of equivalent earthquake cycles Neq	Duration of the earthquake td(s)
3 (Moderate)	5.5	4	8
4 (Average)	6.0	8	14
5 (Strong)	7.5	20	40

Figure 9 represents the results of the pressure meter tests of four boreholes near the project, to be sure we took the minimum value of the pressure meter modulus of the four boreholes:

$$E_{oed} = EM/\dot{\alpha}$$

where:

E_{oed} is the oedometric modulus.

EM is the pressuremeter modulus. $\dot{\alpha}$ is the rheological coefficient of the soil.

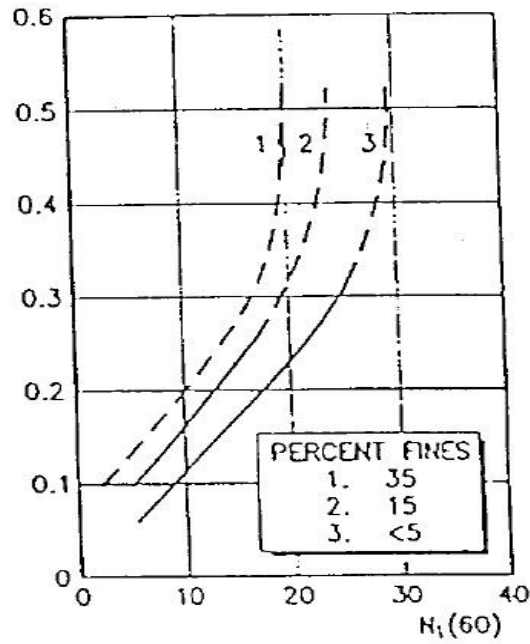


Figure 8.
Number of cycles leading the soil to liquefaction according to the percentage of fine [2].

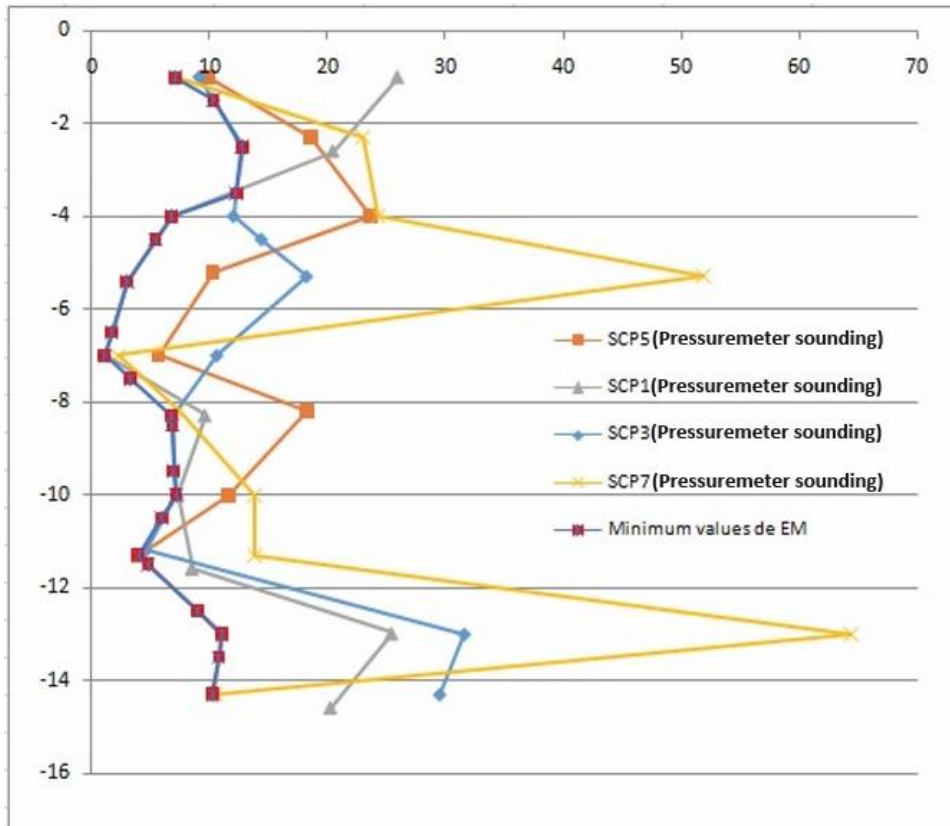


Figure 9.
The pressuremeter module according to the depth in Mpa.

Figure 9 Illustrates The pressuremeter module according to the depth in Mpa.

Table 6.

Evaluation of liquefaction mitigation by stone columns for borehole P1.

Depth	FS	EM (Mpa)	α	Mv (Mpa-1)	Tab	ru max
2.5	0.99	12.8	0.33	0.03	3.39	< 0.6
4.5	1.05	5.45	0.33	0.06	1.45	< 0.6
5.5	0.70	2.95	0.33	0.11	0.78	< 0.6
6.5	0.81	1.7	0.33	0.19	0.45	< 0.6
7.5	0.85	3.3	0.33	0.10	0.88	< 0.6
8.5	0.68	6.85	0.33	0.05	1.82	< 0.6
9.5	0.75	6.96	0.33	0.05	1.85	< 0.6
10.5	0.74	5.96	0.33	0.06	1.58	< 0.6
11.5	0.71	4.84	0.33	0.07	1.28	< 0.6
12.5	0.68	9.01	0.33	0.04	2.39	< 0.6
13.5	0.71	10.8	0.33	0.03	2.86	< 0.6
14.5	0.72	10.3	0.33	0.03	2.73	< 0.6
15.5	0.94	10.3	0.33	0.03	2.73	< 0.6
16.5	1.03	10.3	0.33	0.03	2.73	< 0.6
17.5	0.93	10.3	0.33	0.03	2.73	< 0.6

Note :((FS): Factor safety) , (EM : Pressuremeter module), (α : Rheological coefficient of the soil), (mv : Soil compressibility), (Tab: Dimensionless parameter),(rumax = $U / v0' < 0.6$ (U: Interstitial pressure, v0': Initial effective stress).

According to Table 6, ru max is much less than 0.6, so the risk of liquefaction of the soils of the liquefiable depths is solved, hence the effectiveness of the treatment. Therefore, a square mesh of stone columns spaced 2.5 m apart can eliminate the risk of liquefaction in this area.

5. Analysis and Discussions

The three post-liquefaction settlement prediction methods presented in the previous section Figure 5 (the Post-liquefaction settlement for the 11 boreholes for the three methods) give values that are in agreement with each other with a slight difference. By observing the results of the calculations, we notice that for the majority of the values, the calculation method of the Slake program is the most conservative, providing higher post-liquefaction settlement values for the majority of the boreholes. While the two methods Zhang, et al. [13] and Dhouib and Blondeau [16] give almost the same values. For the liquefaction potential, the three methods give almost the same results.

By analyzing the results of the post-liquefaction settlement and the liquefaction potential, a linear relationship can be established between the two quantities using the least squares method.

Based on in situ tests, the installation of 0.8m stone columns spaced at a maximum of 2.5m can solve the problem of soil liquefaction.

6. Conclusion

The Souani area in the city of Al Hoceima is characterized by the existence of sandy deposits. This study presents a guideline to focus on the problems of these soils, in particular the risk of liquefaction. Based on in situ tests, it was confirmed that this area presents a risk of soil liquefaction at depths of up to 18 m.

Given the high proportions of fines in the soils, which represent more than 10%, vibro-compaction alone cannot constitute the treatment of this soil, thus the installation of stone columns 0.8m apart and spaced 2.5m up to the depth of 18m is mandatory. This treatment could ward off the liquefaction of the soil.

References

- [1] T. L. Youd and I. M. Idriss, "Liquefaction resistance of soils: Summary report from the 1996 NCEER and 1998 NCEER/NSF workshops on evaluation of liquefaction resistance of soils," *Journal of Geotechnical and Geoenvironmental Engineering*, vol. 127, no. 4, pp. 297-313, 2001. [https://doi.org/10.1061/\(asce\)1090-0241\(2001\)127:4\(297\)](https://doi.org/10.1061/(asce)1090-0241(2001)127:4(297))
- [2] EN 1998-5, "(English): Eurocode 8: Design of structures for earthquake resistance – Part 5: Foundations, retaining structures and geotechnical aspects [Authority: The European Union Per Regulation 305/2011, Directive 98/34/EC, Directive 2004/18/EC]. Retrieved from: <https://www.phd.eng.br/wp-content/uploads/2014/11/en.1998.5.2014.pdf>," 2004.
- [3] RPS, "The RPS 2000 seismic building regulations, 2011 version, department of quality and technical affairs, ministry of housing and urban policy in Morocco. Retrieved from: <https://www.academia.edu/33259147>," 2000.
- [4] H. B. Seed and I. M. Idriss, "Simplified procedure for evaluating soil liquefaction potential," *Journal of the Soil Mechanics and Foundations Division*, vol. 97, no. 9, pp. 1249-1273, 1971. <https://doi.org/10.1061/jsfeaq.0001662>
- [5] S. S. C. Liao and R. V. Whitman, *A catalog of liquefaction and Non-liquefaction occurrences during earthquakes, department of civil engineering*. Cambridge, MA: Massachusetts Institute of Technology, 1986.
- [6] I. M. Idriss and R. W. Boulanger, "Soil liquefaction during earthquakes," Monograph MNO-12, Earthquake Engineering Research Institute, Oakland, CA, 261, 2008.
- [7] I. M. Idriss and R. W. Boulanger, *SPT - based liquefaction triggering procedure, centre for geotechnical modeling, department of civil and environmental engineering*. California: Universitu of California, Davis, 2010.
- [8] I. Idriss and R. Boulanger, "Semi-empirical procedures for evaluating liquefaction potential during earthquakes," *Soil Dynamics and Earthquake Engineering*, vol. 26, no. 2-4, pp. 115-130, 2006. <https://doi.org/10.1016/j.soildyn.2004.11.023>

- [9] I. M. Idriss and R. W. Boulanger, "Semi-empirical procedures for evaluating liquefaction potential during earthquakes," presented at the 11th International Conference on Soil Dynamics and Earthquake Engineering, and 3rd International Conf. on Earthquake Geotechnical Engineering, Berkeley, USA: 32–56), 2004.
- [10] K. Tokimatsu and H. B. Seed, "Evaluation of settlements in sands due to earthquake shaking," *Journal of Geotechnical Engineering*, vol. 113, no. 8, pp. 861-878, 1987. [https://doi.org/10.1061/\(asce\)0733-9410\(1987\)113:8\(861\)](https://doi.org/10.1061/(asce)0733-9410(1987)113:8(861))
- [11] K. Ishihara and M. Yoshimine, "Evaluation of settlements in sand deposits following liquefaction during earthquakes," *Soils and Foundations*, vol. 32, no. 1, pp. 173-188, 1992. <https://doi.org/10.3208/sandf1972.32.173>
- [12] E. Javelaud, "Implementation of the graded approach in liquefaction studies," in *Proceedings of the 9th National Days of Geotechnics and Engineering Geology*, 2016.
- [13] G. Zhang, P. Robertson, and R. W. Brachman, "Estimating liquefaction-induced ground settlements from CPT for level ground," *Canadian Geotechnical Journal*, vol. 39, no. 5, pp. 1168-1180, 2002. <https://doi.org/10.1139/t02-047>
- [14] AFPS, "Technical Notebook 45 : Assessment of the risk of soil liquefaction under the effect of earthquakes: Practical knowledge and applications to geotechnical projects. CT45 - December 2020, (The French Association of Paraseismic Engineering)," 2020.
- [15] T. Iwasaki, K. Tokida, and F. Tatsuoka, "Soil liquefaction potential evaluation with use of the simplified procedure," presented at the First International Conference on Recent Advances in Geotechnical Earthquake Engineering and Soil Dynamics, 1981.
- [16] A. Dhouib and F. Blondeau, "Stone columns - implementation techniques, fields of application, behavior, justifications, lines of research and development: Presses of the National School of Bridges and Roads, 2004/ Presses of the National School of Bridges and Roads. Retrieved from: https://www.lavoisier.fr/livre/autre/colonnes-ballastees/dhouib/descriptif_2205262," 2005.
- [17] M. R. Madhav and J. N. Arlekar, "Dilation of granular piles in mitigating liquefaction of sand deposits," in *12th World Conference Earthquake Engineering*, 2000, p. 1035.
- [18] H. B. Seed and J. R. Booker, "Stabilization of potentially liquefiable sand deposits using gravel drains," *Journal of the Geotechnical Engineering Division*, vol. 103, no. 7, pp. 757-768, 1977. <https://doi.org/10.1061/ajgeb6.0000453>
- [19] S. K. Lambert, "Fondations spéciales, evaluation of the risk reduction of liquefaction by stone columns," in *Proceeding of the 18th International Conference on Soil Mechanics and Geotechnical Engineering, Paris*, 2013.
- [20] J. R. Booker, M. S. Rahman, and H. B. Seed, "GADFLEA—A computer program for the analysis of pore pressure generation and dissipation during cyclic or earthquake loading," Rep. No. EERC 76–24, Univ. of California at Berkeley, Berkeley, Calif, 1976.